ON THE DETECTION OF NON-STATIONARY SIGNALS IN THE MATCHED SIGNAL TRANSFORM DOMAIN

Andrei Anghel[†⋆] *Gabriel Vasile*[†] *Cornel Ioana*[†] *Remus Cacoveanu*[⋆] *Silviu Ciochina*[⋆]

[†] Grenoble INP / CNRS, Grenoble-Image-sPeech-Signal-Automatics Lab (GIPSA-lab)
11 rue des Mathematiques, Grenoble Campus, 38402 Saint Martin d'Heres Cedex, FRANCE
[⋆] University Politehnica of Bucharest, 1-3 Iuliu Maniu, 061071 Bucharest, ROMANIA

ABSTRACT

This paper proposes a detector of multi-component non-stationary signals based on the matched signal transform (MST). In the MST domain, a non-stationary signal is localized at its frequency modulation rate with the transform's basis modulation function. The MST can be numerically implemented either as a freestanding discrete version of an integral transform, or for faster computation, as a time resampled version of the original signal followed by a fast Fourier transform. We analyze the noise statistics in the MST domain and derive the analytical forms of the probability density function for both implementations, considering the non-stationary signal embedded in white Gaussian noise. We propose a detector based on the squared magnitude of the MST and show how its detection performances depend on the chosen implementation. All the theoretical derivations are validated through Monte Carlo simulations.

***Index Terms*—** Detection; Non-stationary signals; Time resampling; Time-frequency analysis.

1. INTRODUCTION

The spectral content of signals acquired in real applications like radar or under-water acoustics is usually non-stationary in the sense that the instantaneous frequencies vary in time. This type of signals require specific analysis tools in order to estimate and detect their specific time-frequency structure.

When there is no prior information about the phase law of a non-stationary signal, a widely used model is the polynomial phase signal (PPS). A classical parameters estimation method for the polynomial parameters of PPSs is based on the high-order ambiguity function (HAF) [1, 2] and its upgraded versions more suited for multi-component signals -the product HAF [3] and the warped HAF [4]. If the time-frequency shape of each component is known and can be described by a certain basis function, the modulation rates of the components can be obtained by employing the matched signal transform (MST) [5, 6] or, equivalently, applying a time warping of the signal with the basis function followed by a Fourier transform (FT). In the MST domain, non-stationary signals are localized at their frequency modulation (FM) rates in a similar manner as a sinusoid is localized at its frequency by a spectral representation. For the case when the phase law is partially known, we have proposed in [7] a model-based parameters estimation method designed for non-stationary components having the basis function described by the same model with a few unknown parameters.

While the representation and parameters estimation of non-stationary signals are analyzed in several works, the matter of detecting a non-stationary signal embedded in noise, after applying a certain signal-adapted processing tool is usually addressed in literature only as an extension to the posed representation or estimation problem. For instance, in [8] is proposed an adaptive detection method of PPSs embedded in white Gaussian noise that uses the product HAF, whereas several PPSs detection methods based on time-frequency representations are presented in [9, 10, 11, 12].

In the case of the MST, or time warping followed by an FT, there is no discussion in the literature about the statistical detection of signals in this transformed representation domain. Therefore, in this paper we analyze the noise statistics in the MST domain and propose a detection scheme for non-stationary signals embedded in complex white Gaussian noise processed through two discrete implementations of the MST -direct computation and time resampling. We particularize the results for real and circular noises, which in practical terms correspond to signals obtained from receivers with one channel and two channels in quadrature, respectively. The upgrade of the MST processing technique with a statistically characterized detector is essential for its applications in radar [13] and communications [6].

The remainder of the paper is structured as follows. Section II shows in several steps the analytical derivation of the probability density function of the noise in the discrete MST domain, while Section III presents the detection scheme. In Section IV we present a numerical validation of the theoretical developments, whereas Section V concludes the paper.

2. ANALYTICAL DEVELOPMENT

2.1. Time warping and the matched signal transform

We consider a deterministic signal consisting of a sum of M non-stationary components, each having the same time-frequency shape described by a monotonic one-to-one function of time $\theta(t)$ (a basis function) defined on the interval $[0, T]$. Such a signal can be expressed as

$$s(t) = \sum_{m=1}^{M} A_m \exp\left(j2\pi\alpha_m\theta(t)\right), \tag{1}$$

where A_m and α_m are respectively the complex amplitude and modulation rate of component m. There is no weighing window considered for derivations simplicity. If the signal in (1) is viewed in a warped time axis $\theta = \theta(t)$, it will appear as a signal composed of a sum of complex sinusoids

$$s_{warp}(\theta) = \sum_{m=1}^{M} A_m \exp\left(j2\pi\alpha_m\theta\right). \tag{2}$$

The Fourier transform of (2)

$$S(\alpha) = \int_{\theta(0)}^{\theta(T)} s_{warp}(\theta) \exp\left(-j2\pi\alpha\theta\right) d\theta \tag{3}$$

will give peaks at the modulation rates α_m of the M components. The transform in (3) can also be computed in terms of the initial time axis t as a modified form of the MST defined in [6] applied for the function $\theta(t)$

$$S_{MST}(\alpha) = \int_0^T |\theta'(t)| s(t) \exp\left(-j2\pi\alpha\theta(t)\right) dt. \tag{4}$$

In the following sections we will show that from the implementation point of view, the two ways of evaluating the Fourier transform of a time warped signal may deliver different results in the presence of noise.

2.2. Discrete signal model

The discrete form $s[n]$ of the signal in (1), uniformly sampled at N time instants $t_0, t_1, ..., t_{N-1}$ embedded in a complex white Gaussian noise $w[n] = w_R[n] + jw_I[n]$ is expressed as

$$x[n] = s[n] + w[n] = \sum_{m=1}^{M} A_m \exp\left(j2\pi\alpha_m\theta(t_n)\right) + w[n]. \tag{5}$$

Both $w_R[n]$ and $w_I[n]$ are zero-mean real Gaussian noises that have the probability density function (PDF)

$$f_1^{(R/I)}(u) = \frac{1}{\sqrt{2\pi}\sigma_{R,I}} \exp\left(-\frac{u^2}{2\sigma_{R/I}^2}\right), \tag{6}$$

where $\sigma_{R/I}^2$ are the variances. The characteristic function (CF) [14] of a continuous random variable having the PDF in (6) is

$$F_1^{(R/I)}(v) = \exp\left(-\frac{\sigma_{R/I}^2 v^2}{2}\right). \tag{7}$$

Although $x[n]$ is complex, in the following derivations we also analyze the case of a real noise, for which $s[n]$ will be considered the real part of the sum of complex exponentials from (5).

2.3. Direct MST implementation

We compute the discrete MST of $x[n]$ at K modulation rates $\alpha_0, \alpha_1, ..., \alpha_{K-1}$ as

$$X_{MST}[k] = \frac{1}{\Theta} \sum_{n=0}^{N-1} |\theta'(t_n)| x[n] \exp\left(-j2\pi\alpha_k\theta(t_n)\right), \tag{8}$$

where $\Theta = \sum_{n=0}^{N-1} |\theta'(t_n)|$ is used to compensate the effect of the amplitude weighing of $x[n]$ (to obtain peak values equal to the actual amplitudes). Since the result of applying the MST to the deterministic signal $s[n]$ was previously explained, in the following we focus on its effect on the noise samples. The MST of the complex noise can be written as follows

$$\begin{aligned} W_{MST}[k] = &\sum_{n=0}^{N-1} w_R[n] \frac{1}{\Theta} |\theta'(t_n)| \cos\left(2\pi\alpha_k\theta(t_n)\right) \\ &+ \sum_{n=0}^{N-1} w_I[n] \frac{1}{\Theta} |\theta'(t_n)| \sin\left(2\pi\alpha_k\theta(t_n)\right) \\ &- j\sum_{n=0}^{N-1} w_R[n] \frac{1}{\Theta} |\theta'(t_n)| \sin\left(2\pi\alpha_k\theta(t_n)\right) \\ &+ j\sum_{n=0}^{N-1} w_I[n] \frac{1}{\Theta} |\theta'(t_n)| \cos\left(2\pi\alpha_k\theta(t_n)\right). \end{aligned} \tag{9}$$

Note that the real and imaginary parts of a sample $W_{MST}[k]$ are a weighted sum of the initial noise samples. Each summation term is a noise sample (a realization of a random variable) multiplied by a different value at every time instant t_n. In order to compute the PDF of the resulting variable $W_{MST}[k]$, we employ two classical results from random variable theory [15, 16] given in the following lines. First, the PDF of the variable obtained by multiplying a random variable having the PDF $f(u)$ and CF $F(v)$ with a certain real constant a is given by

$$f_a(u) = \frac{1}{|a|} f_w\left(\frac{u}{a}\right), \tag{10}$$

and the corresponding CF is

$$F_a(v) = F(av). \tag{11}$$

Second, the CF of a sum of independent random variables is given by the product of their CFs. Therefore, the CFs of the real and imaginary parts of the variable $W_{MST}[k]$ are

$$\begin{aligned} F_{MST}^{(R/I)}(v,k) = \exp\Bigg\{ &-\frac{v^2}{2}\sum_{n=0}^{N-1} |\theta'(t_n)|^2 \\ &\times \left[\frac{\sigma_{R,I}^2}{\Theta^2}\cos^2\left(2\pi\alpha_k\theta(t_n)\right) + \frac{\sigma_{I,R}^2}{\Theta^2}\sin^2\left(2\pi\alpha_k\theta(t_n)\right)\right]\Bigg\}. \end{aligned} \tag{12}$$

By analyzing the structure of (12), we can see that $W_{R,MST}[k]$ and $W_{I,MST}[k]$ have a Gaussian distribution with the variance depending on the index k. Next, we compute the variances of the resulting variables for two particular cases. If we consider a real noise ($\sigma_R = \sigma$ and $\sigma_I = 0$), the variance of the MST samples (real and imaginary) is expressed as

$$\sigma_{MST,R/I}^2[k] = \frac{\sigma^2}{\Theta^2} \sum_{n=0}^{N-1} |\theta'(t_n)|^2 \{\text{cos/sin}\}^2 \left(2\pi\alpha_k\theta(t_n)\right), \tag{13}$$

while for a circular noise ($\sigma_R = \sigma_I = \sigma$) the variances of the real and imaginary parts are equal and do not depend on the index k:

$$\sigma_{MST,C}^2 = \frac{\sigma^2}{\Theta^2} \sum_{n=0}^{N-1} |\theta'(t_n)|^2. \tag{14}$$

Note that when $\theta'(t) = t$ the MST transforms in a Fourier transform and the variances for both noise types become $\sigma_{FFT}^2 = \sigma^2/N$.

2.4. Time resampling MST implementation

In the warped time axis θ, the samples of $x[n]$ are related to the time instants $\theta(t_n)$, which leads to a non-uniformly sampled signal. Hence, the computation of the Fourier transform of $x[n]$ in the θ time axis can be efficiently implemented by a resampling of the initial signal (to obtain a uniformly sampled signal) followed by a Fast Fourier Transform (FFT). The MST of signal $x[n]$ computed by time resampling will be denoted as $X_{RS}[k]$.

In this subsection we compute the PDF of the MST samples for the noise $w[n]$ using the discrete version of (1) and considering that the resampling is employed by the nearest neighbor interpolation. Although the high-order spline functions are more suited for resampling [17], the nearest neighbor suffices for the theoretical purpose of the paper and was chosen due to analytical calculation simplicity.

We denote with $\zeta[n]$ the resampled noise signal at the moments $\theta_0, \theta_1, ..., \theta_{N-1}$. The Fourier transform of the resampled noise is

$$W_{RS}[k] = \frac{1}{N} \sum_{n=0}^{N-1} \zeta[n] \exp\left(-j2\pi\alpha_k\theta_n\right). \tag{15}$$

In the case of nearest neighbor interpolation, each $\zeta[n]$ will be one of the original samples $w[n]$. The linking between the two sets of samples depends on the actual basis function $\theta(t)$. Some of the samples $w[n]$ may be left out and some may appear for more than one index n, so two random variables whose realizations are $\zeta_R[n_1]$ and $\zeta_R[n_2]$ (or $\zeta_I[n_1]$ and $\zeta_I[n_2]$) are either identical or independent.

We define an indexing matrix $\beta[n,l]$ which links the N original samples to the N resampled ones. Matrix β has N lines, and the number of columns is given by the maximum number of repetitions of an original sample in the resampled signal. The number of repetitions of sample n is denoted $\iota[n]$, and therefore line n of the matrix will have $\iota[n]$ indices followed by zeros. With these notations, equation (15) can be rewritten as

$$\begin{aligned} W_{RS}[k] &= \sum_{n=0}^{N-1} w_R[n]\frac{1}{N}\sum_{l=0}^{\iota[n]-1}\cos\left(2\pi\alpha_k\theta_{\beta[n,l]}\right)\\ &+\sum_{n=0}^{N-1} w_I[n]\frac{1}{N}\sum_{l=0}^{\iota[n]-1}\sin\left(2\pi\alpha_k\theta_{\beta[n,l]}\right)\\ &-j\sum_{n=0}^{N-1} w_R[n]\frac{1}{N}\sum_{l=0}^{\iota[n]-1}\sin\left(2\pi\alpha_k\theta_{\beta[n,l]}\right)\\ &+j\sum_{n=0}^{N-1} w_I[n]\frac{1}{N}\sum_{l=0}^{\iota[n]-1}\cos\left(2\pi\alpha_k\theta_{\beta[n,l]}\right). \end{aligned} \tag{16}$$

Notice that $\beta[n,l]$ has to be numerically evaluated from case to case because it comes from the actual linking between the initial and resampled set of samples for the given $\theta(t)$. Additionally, it can be shown using (16) that the peak values of the MST computed by resampling may be biased relative to the actual amplitude A_m of the matched signal in the time domain. For a more accurate type of interpolation, an interpolated sample is a weighted sum of a few original samples and consequently an analytic expression like (16) is much more difficult to derive.

Using the same approach as in the previous section, the real and imaginary parts of $W_{RS}[k]$ will have the CFs:

$$\begin{aligned} F_{RS}^{(R/I)}(v,k) = \exp\Bigg\{ &-\frac{v^2}{2}\sum_{n=0}^{N-1}\frac{\sigma^2_{R,I}}{N^2}\left(\sum_{l=0}^{\iota[n]-1}\cos\left(2\pi\alpha_k\theta_{\beta[n,l]}\right)\right)^2\\ &+\frac{\sigma^2_{I,R}}{N^2}\left(\sum_{l=0}^{\iota[n]-1}\sin\left(2\pi\alpha_k\theta_{\beta[n,l]}\right)\right)^2\Bigg\}. \end{aligned} \tag{17}$$

For the particular cases of real noise and circular noise the variances are

$$\sigma^2_{RS,R/I}[k] = \frac{\sigma^2}{N^2}\sum_{n=0}^{N-1}\left(\sum_{l=0}^{\iota[n]-1}\{\text{cos/sin}\}\left(2\pi\alpha_k\theta_{\beta[n,l]}\right)\right)^2, \tag{18}$$

and respectively

$$\begin{aligned} \sigma^2_{RS,C}[k] = \frac{\sigma^2}{N^2}\sum_{n=0}^{N-1}&\left(\sum_{l=0}^{\iota[n]-1}\cos\left(2\pi\alpha_k\theta_{\beta[n,l]}\right)\right)^2\\ &+\left(\sum_{l=0}^{\iota[n]-1}\sin\left(2\pi\alpha_k\theta_{\beta[n,l]}\right)\right)^2. \end{aligned} \tag{19}$$

3. DETECTION IN THE MST DOMAIN

The actual detection in the MST domain is done by peak picking the squared magnitude of $X_{MST}[k]$ or $X_{RS}[k]$ (generically denoted by $X[k]$) and comparing it to a certain threshold. The approach is similar to the detection of sinusoidal signals using the Fourier transform [18]. The expected value of a peak placed at bin k of the MST domain can have two values according to the presence (hypothesis H_1) or absence (hypothesis H_0) of a non-stationary signal with modulation rate α_k:

$$\begin{aligned} H_1 &: E\left\{|X[k]|^2\right\} = |\Delta_k|^2 + \sigma^2_{W,R}[k] + \sigma^2_{W,I}[k],\\ H_0 &: E\left\{|X[k]|^2\right\} = \sigma^2_{W,R}[k] + \sigma^2_{W,I}[k], \end{aligned} \tag{20}$$

where $E\{\}$ is the statistical expectation operator and Δ_k is the complex signal's amplitude in the MST domain (that may be inherently biased relative to A_m for the resampling-based implementation). $\sigma^2_{W,R}[k]$ and $\sigma^2_{W,I}[k]$ are the variances computed in (13), (14), (18) or (19), depending on the implementation and noise type. To obtain a constant false alarm rate (CFAR) detector, the threshold level $\gamma[k]$ has to be adjusted according to the noise statistics in each bin. The envisaged detection scheme is given in Fig. 1.

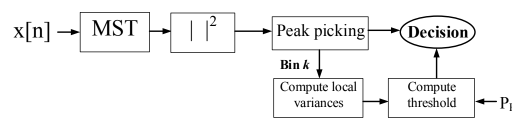

Fig. 1. MST-based detection scheme.

To compute the probability of false alarm (P_F), the PDFs of $|W_{RS}[k]|^2$ and $|W_{MST}[k]|^2$ in each considered case have to be evaluated. It can be shown that the real and imaginary parts of the MST samples of noise are uncorrelated for both $W_{MST}[k]$ and $W_{RS}[k]$ (onwards denoted $W[k] = W_R[k] + jW_I[k]$ when referring to a common characteristic). Next, we consider two results regarding random variables [19]. First, the lack of correlation between two Gaussian variables implies the independence of the two variables. Therefore the noise contribution to $E\left\{|X[k]|^2\right\}$ comes from a sum of two squared independent Gaussian variables (the real and imaginary part of $W[k]$). Second, the sum of n squared independent Gaussian variables with variance σ^2_W has a Gamma distribution with the shape factor $n/2$ and the scale factor $2\sigma^2_W$:

$$f\left(u|\frac{n}{2},2\sigma^2_W\right) = \frac{1}{\Gamma\left(\frac{n}{2}\right)2\sigma^2_W}\left(\frac{u}{2\sigma^2_W}\right)^{\frac{n}{2}-1}\exp\left(-\frac{u}{2\sigma^2_W}\right), \tag{21}$$

where $\Gamma(x)$ is the Gamma function.

In the case of a circular noise, when the variances $\sigma^2_{W,R}[k]$ and $\sigma^2_{W,I}[k]$ are equal to $\sigma^2_W[k]$, and $n=2$, the PDF of $|W[k]|^2$ is

$$f_c(u,k) = f\left(u|1,2\sigma^2_W[k]\right) = \frac{1}{2\sigma^2_W[k]}\exp\left(-\frac{u}{2\sigma^2_W[k]}\right). \tag{22}$$

For a real noise, the variances $\sigma^2_{W,R}[k]$ and $\sigma^2_{W,I}[k]$ are different and the PDF can be obtained as the convolution between the individual PDFs of $|W_R[k]|^2$ and $|W_I[k]|^2$, which are $f\left(u|1/2,2\sigma^2_{W,R}[k]\right)$ and $f\left(u|1/2,2\sigma^2_{W,I}[k]\right)$, respectively. This type of convolution is computed in [16] and the result is:

$$\begin{aligned} f_r(u,k) = \frac{1}{2\sigma_{W,R}[k]\sigma_{W,I}[k]}&\exp\left[-\frac{u}{4}\left(\frac{1}{\sigma^2_{W,R}[k]}+\frac{1}{\sigma^2_{W,I}[k]}\right)\right]\\ &\times I_0\left[\frac{u}{4}\left(\frac{1}{\sigma^2_{W,R}[k]}-\frac{1}{\sigma^2_{W,I}[k]}\right)\right], \end{aligned} \tag{23}$$

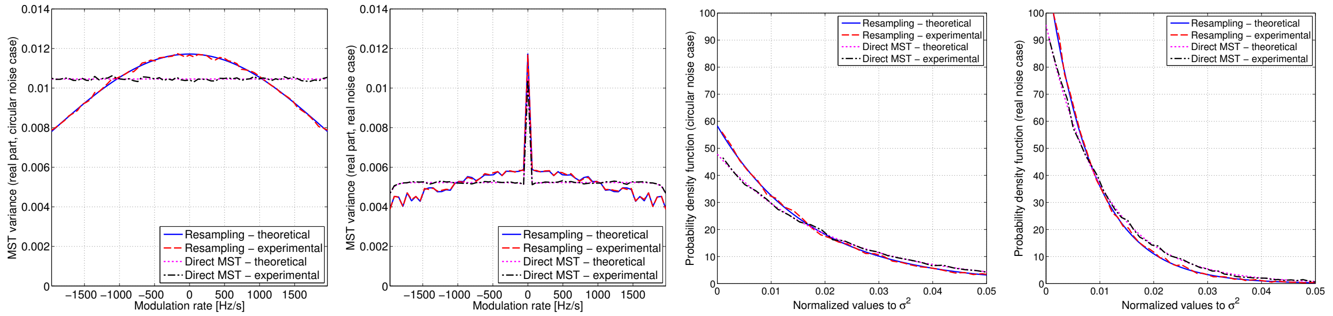

(a) (b) (c) (d)

Fig. 2. Theoretical and experimental results of noise statistics analysis: noise variance of the real part in the MST domain for circular noise (a) and real noise (b), PDF of the MST squared magnitude for circular noise (c) and real noise (d) at 1700 Hz/s modulation rate.

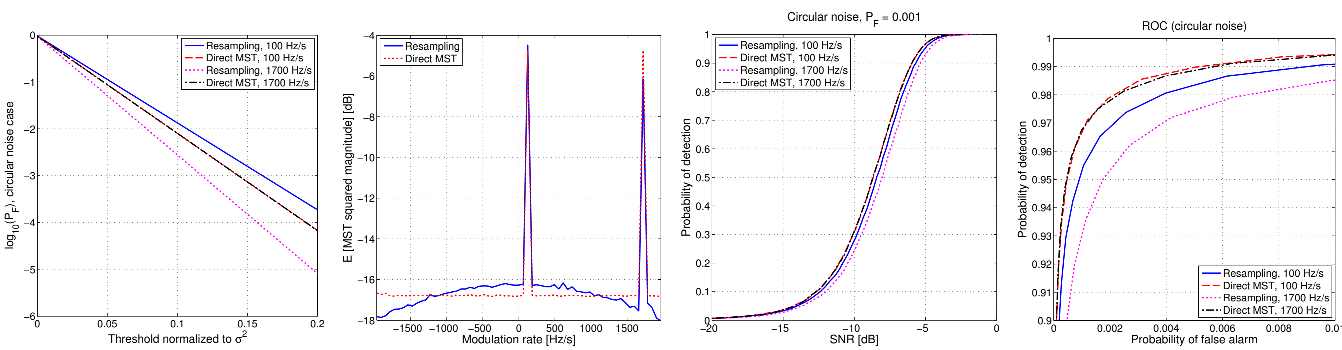

(a) (b) (c) (d)

Fig. 3. MST detector - performance evaluation for a signal composed of two chirps embedded in circular noise: (a) P_F vs. threshold, (b) Expected squared magnitude of the MST, (c) Probability of detection vs. SNR for $P_F = 10^{-3}$, (d) ROC for an SNR $A^2/\sigma^2 = 1/2$.

where $I_0[]$ is the zero order Bessel function.

With these results the P_F can be obtained by numerical integration, while the detection probability depends on the signal's amplitude and doesn't have a straightforward analytic expression.

4. NUMERICAL VALIDATION

In this section we present the results obtained in a set of Monte Carlo simulations used to validate the theoretical developments. We obtained through simulations the variances of the real and imaginary parts of the noise processed through the two implementations of the MST and generated the experimental PDFs of the squared magnitude of the noise samples in the MST domain. The following parameters were considered in the simulations for both real and circular noises: basis function $\theta(t) = t^2$, variance in time domain $\sigma^2 = 1$, 1 kHz sampling frequency, 128 samples and 40000 realizations of each random process. Fig. 2(a) and Fig. 2(b) show the theoretical and experimental variances of the samples in the MST domain (the real part), while in Fig. 2(c) and Fig. 2(d) we present the PDFs for the squared magnitude of the MST. It can be easily noticed that the simulated variances and PDFs are in keeping with the theoretical results (the relative error between the plots is around 1%).

In Fig. 3 we emphasize the performances of the MST detector for two chirp signals with the same amplitude embedded in white Gaussian circular noise. Due to the fluctuations of the variance, the false alarm probabilities for the resampling implementation depend on the modulation rate. Additionally, the amplitude is biased for the component with higher modulation rate (the effect can be compensated with a correction envelope, but this will also increase the noise variance). The combined effect of the variance and amplitude fluctuations on the detection performances can be seen on the plots of detection probability vs. signal-to-noise ratio (SNR) and receiver operating characteristic (ROC) in Fig. 3(c) and Fig. 3(d), respectively. The SNR is computed as the squared amplitude of the signal divided by the noise variance. In the analyzed cases, the direct implementation has better detection results compared to the nearest neighbor resampling method.

5. CONCLUSIONS

In this paper we analyzed the noise statistics in the matched signal transform domain and proposed, for the first time, a detection scheme for non-stationary signals processed with two implementations of the discrete MST. The theoretical developments were validated through numerical simulations. In the considered test cases, the direct implementation was slightly superior in terms of detection performances with respect to the resampling approach. In future work we shall determine the theoretical noise statistics after the MST for better interpolation methods in terms of signal reconstruction and apply the results to radar and ultrasound applications.

6. REFERENCES

[1] S. Peleg and B. Porat, "Estimation and classification of signals with polynomial phase," *IEEE Transactions on Information Theory*, vol. 37, no. 2, pp. 422–430, March 1991.

[2] Y. Wang and G. Zhou, "On the use of high order ambiguity functions for multicomponent polynomial phase signals," *Signal Processing*, vol. 65, no. 2, pp. 283–296, March 1998.

[3] S. Barbarossa, A. Scaglione, and G. B. Giannakis, "Product high-order ambiguity function for multicomponent polynomial-phase signal modeling," *IEEE Transactions on Signal Processing*, vol. 46, no. 3, pp. 691–708, March 1998.

[4] C. Ioana, C. Cornu, and A. Quinquis, "Polynomial phase signal processing via warped high-order ambiguity function," in *Proceedings of the 12th European Signal Processing Conference (EUSIPCO)*, Vienna, Austria, September 2004, pp. 1159–1162.

[5] A. Papandreou-Suppappola, "Generalized time-shift covariant quadratic time-frequency representations with arbitrary group delays," in *Conference Record of the Twenty-Ninth Asilomar Conference on Signals, Systems and Computers*, October 1995, vol. 1, pp. 553–557.

[6] H. Shen and A. Papandreou-Suppappola, "Wideband time-varying interference suppression using matched signal transforms," *IEEE Transactions on Signal Processing*, vol. 53, no. 7, pp. 2607–2612, July 2005.

[7] A. Anghel, G. Vasile, C. Ioana, R. Cacoveanu, and S. Ciochina, "Model-based parameters estimation of non-stationary signals using time warping and a measure of spectral concentration," in *Proceedings of the IEEE International Conference on Acoustics, Speech and Signal Processing (ICASSP)*, South Brisbane, Queensland, Australia, April 2015, pp. 3706–3710.

[8] S. Barbarossa, R. Mameli, and A. Scaglione, "Adaptive detection of polynomial-phase signals embedded in noise using high-order ambiguity functions," in *Conference Record of the Thirty-First Asilomar Conference on Signals, Systems and Computers*, November 1997, vol. 2, pp. 1228–1232.

[9] S. Barbarossa, "Detection and estimation of the instantaneous frequency of polynomial-phase signals by multilinear time-frequency representations," in *Proceedings of the IEEE Signal Processing Workshop on Higher-Order Statistics*, 1993, pp. 168–172.

[10] J. Wang and P. L. Shui, "Nonlinear frequency modulated signal detection based on time-frequency tiling," in *Proceedings of the IEEE 6th Circuits and Systems Symposium on Emerging Technologies: Frontiers of Mobile and Wireless Communication*, May 2004, vol. 2, pp. 409–412.

[11] Y. Li, W. Tang, and Y. Kuang, "A new polynomial phase signal detection algorithm based on the combination of filter bank and short-time Radon-Wigner transform," in *Proceedings of the International Conference on Communications and Mobile Computing (CMC)*, April 2010, vol. 2, pp. 515–519.

[12] A. Bouchikhi, A.-O. Boudraa, J.-C. Cexus, and T. Chonavel, "Analysis of multicomponent LFM signals by Teager Huang-Hough transform," *IEEE Transactions on Aerospace and Electronic Systems*, vol. 50, no. 2, pp. 1222–1233, April 2014.

[13] A. Anghel, G. Vasile, R. Cacoveanu, C. Ioana, and S. Ciochina, "Range autofocusing for FMCW radars using time warping and a spectral concentration measure," in *Proceedings of the IEEE Radar Conference (RadarCon)*, May 2015, pp. 0581–0586.

[14] O. C. Ibe, *Fundamentals of Applied Probability and Random Processes*, Elsevier Academic Press, Burlington, MA, 2005.

[15] R. Durrett, *Probability: Theory and Examples (Cambridge Series in Statistical and Probabilistic Mathematics)*, Cambridge University Press, New York, NY, 2010.

[16] B. Lévine, *Fondements théoriques de la radiotechnique statistique. Tome I*, Edition Mir, Moscow, 1973.

[17] A. Jarrot, C. Ioana, and A. Quinquis, "Toward the use of time-warping principle with discrete-time sequences," *Journal of Computers*, vol. 2, no. 6, pp. 49–55, 2007.

[18] L. Stanković, M. Daković, and T. Thayaparan, *Time-Frequency Signal Analysis with Applications*, Artech House, Boston, 2013.

[19] H. L. Van Trees, K. L. Bell, and Z. Tian, *Detection, Estimation and Modulation Theory. Part I - Detection, Estimation and Filtering Theory*, John Wiley & Sons, Hoboken, NJ, 2013.